Published in final edited form as:

Br J Dermatol. 2017 December ; 177(6): 1601–1611. doi:10.1111/bjd.15716.

Coexistence of Eph receptor B_1 and ephrin B_2 in port-wine stain endothelial progenitor cells contributes to clinicopathological vasculature dilatation

W. Tan[1], **J. Wang**[1,2], **F. Zhou**[1,2], **L. Gao**[1,3], **R. Yin**[1,4], **H. Liu**[5], **A. Sukanthanag**[1], **G. Wang**[3], **M.C. Mihm Jr.**[6], **D.-B. Chen**[7], **J.S. Nelson**[1,8]

[1]Department of Surgery, Beckman Laser Institute and Medical Clinic, University of California, Irvine, Irvine, CA, U.S.A.

[2]The Third Xiangya Hospital, Xiangya School of Medicine, Central South University, Changsha, Hunan 412000, China

[3]Department of Dermatology, Xijing Hospital, Fourth Military Medical University, Xi'an, 710032, China

[4]Department of Dermatology, The Second Hospital of Shanxi Medical University, Taiyuan 030001, China

[5]Shandong Provincial Institute of Dermatology and Venereology, Jinan, Shandong 250022, China

[6]Department of Dermatology, Brigham and Women's Hospital, Harvard Medical School, Boston, MA 02115, U.S.A.

[7]Department of Obstetrics and Gynecology, University of California, Irvine, Irvine, CA, U.S.A.

[8]Department of Biomedical Engineering, University of California, Irvine, Irvine, CA, U.S.A.

Summary

Background—Port-wine stain (PWS) is a vascular malformation characterized by progressive dilatation of postcapillary venules, but the molecular pathogenesis remains obscure.

Objectives—To illustrate that PWS endothelial cells (ECs) present a unique molecular phenotype that leads to pathoanatomical PWS vasculatures.

Methods—Immunohistochemistry and transmission electron microscopy were used to characterize the ultrastructure and molecular phenotypes of PWS blood vessels. Primary culture of human dermal microvascular endothelial cells and *in vitro* tube formation assay were used for confirmative functional studies.

Results—Multiple clinicopathological features of PWS blood vessels during the development and progression of the disease were shown. There were no normal arterioles and venules

Correspondence Wenbin Tan. wenbint@uci.edu.

Conflicts of interest
None declared.

Supporting Information
Additional Supporting Information may be found in the online version of this article at the publisher's website:

observed phenotypically and morphologically in PWS skin; arterioles and venules both showed differentiation impairments, resulting in a reduction of arteriole-like vasculatures and defects in capillary loop formation in PWS lesions. PWS ECs showed stemness properties with expression of endothelial progenitor cell markers CD133 and CD166 in non-nodular lesions. They also expressed dual venous/arterial identities, Eph receptor B1 (EphB1) and ephrin B2 (EfnB2). Co-expression of EphB1 and EfnB2 in normal human dermal microvascular ECs led to the formation of PWS-like vasculatures *in vitro*, for example larger-diameter and thick-walled capillaries.

Conclusions—PWS ECs are differentiation-impaired, late-stage endothelial progenitor cells with a specific phenotype of $CD133^+/CD166^+/EphB1^+/EfnB2^+$, which form immature venule-like pathoanatomical vasculatures. The disruption of normal EC–EC interactions by coexistence of EphB1 and EfnB2 contributes to progressive dilatation of PWS vasculatures.

Port-wine stain (PWS) is a congenital progressive vascular malformation of human skin, involving the dermal superficial vascular plexus, with an estimated prevalence of 3–5 children per 1000 live births.[1,2] PWS initially appears as flat, red macules in childhood; lesions tend to darken progressively to purple and by middle age they often become raised as a result of the development of vascular nodules, which are susceptible to spontaneous bleeding or haemorrhage.[3,4] As most malformations occur on the face, PWS is also a significant clinical problem that results in loss of self-esteem.[5–7] The pulsed-dye laser (PDL) is the treatment choice for PWS, but the regrowth of clinicopathological blood vessels post-PDL is a major clinical barrier that needs to be overcome.[8–10] PWS is usually characterized by a dilatation of postcapillary venules based on morphological observations.[11] Recent studies have suggested that the sporadic somatic mutation of GNAQ (c.548G > A) is linked to PWS.[12,13] The GNAQ (c.548G > A) mutation is primarily present in blood vessels.[14,15] In addition, PWS has sustained activation of mitogen-activated protein kinases.[16] However, the pathogenesis of PWS remains incompletely understood.

We hypothesize that PWS endothelial cells (ECs) are differentiation-impaired endothelial progenitor cells (EPCs), consisting of a dermal primitive capillary plexus (PCP), which eventually develop into venule-like vasculatures morphologically; and that co-expression of venous and arterial-specific markers, for example Eph receptor B1 (EphB1) and ephrin B2 (EfnB2), in PWS EPCs disrupts normal EC–EC interactions, leading to the progressive dilatation of PWS vasculatures observed over time.

Materials and methods

Tissue preparation

The study was approved by the Institutional Review Board at the University of California, Irvine. A total of 37 PWS biopsy samples, including four infant, 11 paediatric, five teenage and 17 adult specimens, were obtained from 27 subjects and de-identified for this study (Table 1). A total of 14 infantile, 40 paediatric, 43 teenage and 45 adult control skin specimens from adjacent normal skin or patients without PWS were retrieved from skin biopsy tissue banks at our departments and served as controls. Biopsy tissue was fixed in 10% buffered formalin (Fisher Scientific, Pittsburgh, PA, U.S.A.) and processed for permanent paraffin embedding on an ASP 300 tissue processor (Leica Microsystems,

Bannockburn, IL, U.S.A.). Approximately 6-μm-thick paraffin sections were cut and collected.

For blood vessel counting, six of 600 μm × 300 μm or two of 1200 μm × 600 μm areas underneath the epidermis in each biopsy section were randomly picked. The numbers and perimeters of blood vessels in each chosen area were counted and measured. A total of 464 normal blood vessels (n = 11 control subjects) and 982 lesional blood vessels (n = 15 patients with PWS) were analysed. The total numbers of rete ridges and papillae containing capillary loops from each section were counted and the full length of epidermis of each section was directly measured using Nikon NIS-Elements software (Nikon, Tokyo, Japan). The densities of rete ridges and papillae containing capillary loops per mm epidermis were calculated. The number of participants in each age group is listed in Table 2. The arteriole-like and venule-like vasculatures were identified based on their morphological characteristics from semi-thin sections from infants with PWS (n = 4).[17] Adjacent normal skin from the same participants were used as controls. A total of 45 PWS and 33 normal blood vessels were identified, counted and categorized. The thickness of blood vessel walls was measured with ImageJ software (National Institutes of Health, Bethesda, MD, U.S.A.).

Semi-thin and ultrathin section preparation

Biopsies were immediately fixed in Karnovsky solution (2% paraformaldehyde, 3% glutaraldehyde, 0·1 mol L^{-1} sodium cacodylate) for 3 h, then underwent postfixation with 1% osmium tetraoxide solution for 1 h, en bloc staining with Kelenberger uranyl acetate buffer for 2 h and a series of dehydrations (30%, 50%, 70%, 90%, 100% ethanol, two-thirds ethanol and one-third propylene oxide, one-third ethanol and two-thirds propylene oxide, and 100% propylene oxide). Tissues then were infiltrated with an Epon mixture overnight and embedded in Epon in a 60 °C oven for 3 days. For light microscopy experiments, the semi-thin sections with thicknesses of 500–600 nm were cut and stained with Richardson solution. For transmission electron microscopy experiments, 70-nm-thick sections were cut and stained with uranyl and lead citrates.

Immunohistochemistry

Paraffin sections were deparaffinized according to routine procedures. Antigen retrieval was performed in 10 mmol L^{-1} sodium citrate buffer (pH 6·0) at 97 °C for 2–4 h. The sections were then incubated in a humidified chamber overnight at 4 °C with the following primary antibodies: CD31 (1 : 50 dilution; Bethyl Laboratories, Montgomery, TX, U.S.A.); CD133 (1 : 50 dilution; Boster Immunoleader, Pleasanton, CA, U.S.A.); von Willebrand factor [vWF; 1 : 50 dilution (Dako, Carpinteria, CA, U.S.A.)]; EphB4 (1 : 50 dilution; Thermo Fisher, Waltham, MA, U.S.A.); CD166, Efn-B2 and EphB1 (all 1 : 50 dilution; all from Santa Cruz Biotechnology, Santa Cruz, CA, U.S.A.). Biotinylated antimouse, antirabbit and antigoat secondary antibodies were incubated with sections for 2 h at room temperature after the primary antibody reactions. An indirect biotin avidin diaminobenzidine (DAB) system (Dako, Glostrup, Denmark) was used for detection.

The cellular immunoreactivity score was evaluated using a system reported by Populo *et al.*[18] Briefly, the intensity was graded as follows: no staining, 0; weak staining, 1;

intermediate staining, 2; strong staining, 3. The percentage of immunoreactive cells was graded as either focal (1 indicates ≤ 30%) or diffuse (2 indicates > 30%). For each antibody, an immunoreactivity score was estimated by multiplying the intensity grade by the grade of the immunoreactive cell percentage. Immunoreactivity scores were classified as follows: negative = 0, low = 1, moderate = 2, 3 and 4, high = 6.

Human dermal microvascular endothelial cell culture

Human dermal microvascular endothelial cells (hDMVECs) were purchased from Cell Applications (San Diego, CA, U.S.A.) and were cultured in EC Basal Medium with growth supplement (Cell Applications). As hDMVECs were a heterogeneous population of venular and arteriolar ECs, we used biotinylated chimera EfnB2–Fc and streptavidin-conjugated magnetic beads to isolate the $EphB1^{+}/EfnB2^{-}$ hDMVEC subpopulation. Chimera EfnB2–Fc (20 μg; R&D Systems, Minneapolis, MN, U.S.A.) was added into a *N*-hydroxysuccinimide type of biotinylation reagent (Thermo Fisher) at a biotin : protein molar ratio of 20 : 1. The reaction was incubated on ice for 2 h. The protein concentration of biotinylated chimera EfnB2–Fc was then determined after desalting or dialysis. For isolation of the $EphB1^{+}/EfnB2^{-}$ hDMVEC subpopulation, biotinylated chimera EfnB2–Fc (2 μg) was first incubated with 100 μg streptavidin-conjugated Sera-Mag magnetic beads (GE Health-care, Pittsburgh, PA, U.S.A.) at room temperature for 15 min; the EfnB2–Fc–magnetic bead complex was then pulled down by magnetic strands to remove free biotinylated chimera EfnB2–Fc. The prepared chimera EfnB2–Fc–magnetic beads were then incubated with 5×10^5 hDMVECs on ice for 30 min. The hDMVEC chimera EfnB2–Fc–magnetic bead complexes were then washed in phosphate-buffered saline three times and cultured in complete EC medium. The selected subpopulation was designated $EphB1^{+}/EfnB2^{-}$ hDMVEC. A total of four independent preparations of a selection of $EphB1^{+}/EfnB2^{-}$ hDMVECs were performed.

Transfection, immunoprecipitation and immunoblot

Human EfnB2 cDNA was amplified using two primers (5'GGCGGATCCATGGATTACAA GGATGACGACGATAAGGCTG TGAGAAGGGACTCCGTG-3' and 5' GGCCTCGAGTC AGT GGTGATGGTGATGATGGTGATGATGGACCTTGTAGTAAATGTTCGC3') to have a Flag and His tag flanked at the N-terminal and C-terminal of EfnB2, respectively. The amplified fragment was cleaved by BamHI and XhoI and cloned into the same sites in a pcDNA3 vector. Insertion was confirmed by Sanger sequencing.

The plasmids containing enhanced green fluorescent protein (EGFP) and human EfnB2 cDNA were transfected into four independently prepared $EphB1^{+}/EfnB2^{-}$ hDMVEC subpopulations by using a FuGene HD (Thermo Fisher). The cells were then screened with G418 (300–600 μg mL^{-1}) for 1 week–10 days to remove untransfected cells in order to obtain $EGFP^{+}/EphB1^{+}/EfnB2^{-}$ and $EphB1^{+}/EfnB2^{-}$ cell models ($n = 4$ for each cell model). For the immunoprecipitation assay, the cells were lysed in RIPA buffer [25 mmol L^{-1} Tris (pH 7–8), 150 mmol L^{-1} NaCl, 0·1% sodium dodecyl sulfate, 0·5% sodium deoxycholate and 1% Triton X-100] with proteinase inhibitors. The cell lysate (50 μg total protein) was precleared by protein G agarose beads and goat IgG (Santa Cruz Biotechnology). Goat anti-EphB1 antibody (0·2 μg; Santa Cruz Biotechnology) was incubated with cell lysate for 2 h at room temperature and followed by addition of 20 μL protein G agarose beads. The

immunoprecipitated components were identified by Western blot using anti-EphB1, EfnB2 and His antibodies.

Matrigel *in vitro* tube formation

The capillary-like structure (CLS) formation of angiogenesis from ECs can be modelled *in vitro* by a Matrigel-based tube formation assay (Thermo Fisher).[19,20] ECs plated on Matrigel at low densities form a network of branching structures, which can be photographed and quantified by measuring the length, perimeter or area of the CLS.[19,20] Matrigel *in vitro* tube formation was performed in 48-well plates. Briefly, Matrigel (80 μL per well, Thermo Fisher) was added to a 48-well plate and incubated at 37 °C for 30 min. hDMVECs (n = 4 for each cell model prepared as described above) were trypsinized and resuspended in EC basal medium without supplements. Each type of cell (2·5–4 9 10^4 in 200 μl) was then added into each well and incubated at 37°C with 5% CO_2 for 12–16 h to form a CLS. The cells were fixed with 4% buffered formalin at the end of the experiments. Images were acquired using a Nikon Eclipse Ti-E system. The CLS wall thickness, perimeter and area of branching point were outlined from the acquired images and directly measured with Nikon NIS-Elements software. The total sample sizes for capillary wall thickness were 47, 46 and 18 CLSs, perimeters were 35, 33 and 12 CLSs, and area of branching points were 155, 79 and 24 CLSs.

Statistics

Paired-samples t-tests were performed to evaluate the statistical differences in CLS morphological parameters among the various cell models, and differences between PWS and normal control datasets. Data are presented as mean ± SD and a P-value < 0·05 was considered significant.

Results

The clinical history of PWS biopsy samples is listed in Table 1. Both ectatic thin- and thick-walled blood vessels were observed in adult PWS lesions (Fig. 1a–c). The density of dermal blood vessels per mm^2 was significantly higher in PWS lesions compared with normal control skins [PWS 53·14 ± 21·16 (n = 982 blood vessels from 15 participants); control 42·22 5·14 (n = 464 blood vessels from 11 participants); P = 0·046]. Adult PWS blood vessels displayed statistically significant dilatation: 50% of PWS blood vessels had a circumference ranging from 50 to 200 μm with an additional 19% ranging from 401 to 2500 μm, whereas only 34% of blood vessels in normal skin had circumferences > 50 μm (n = 982 blood vessels from 15 participants with PWS and 464 blood vessels from 11 controls; P < 0·05, Mann–Whitney U-test; Fig. 1d). However, only ectatic thick-walled, but not thin-walled, blood vessels were observed in infant PWS lesions. Infant PWS blood vessels showed a significantly thicker blood vessel wall compared with adjacent normal skin dermal blood vessels from the same subjects (n = 45 PWS and 33 normal blood vessels from four subjects; P < 0·05) (Fig. 1e–g). These results suggested that ectatic thick-walled rather than thin-walled blood vessels were the primary pathological phenotypes during the early development of PWS.

We next attempted to characterize the arterial/venous pathoanatomical features of PWS blood vessels. Differentiation of veins and arteries from dermal PCP is initiated by the end of the second trimester during normal human embryogenesis.[21] In a normal skin papillary plexus, an arterial capillary wall shows homogeneous-appearing basement membrane material, which is distinguished from venous capillary walls by the presence of multilayered basement membrane and bridged fenestrations.[17] In infant PWS, blood vessels showed dilatations and exhibited a typical venule-like vasculature. We found a substantial reduction in the number of arteriole-like structures in PWS (Fig. 2a, b). The ratio of arteriole-like to venule-like structures observed from semi-thin sections in infant PWS significantly decreased compared with adjacent normal skin from the same subject [PWS 9·17 ± 9·50%; control 61·27 ± 4·89% (n = 45 PWS and 33 normal blood vessels from four subjects); $P < 0·01$] (Fig. 2c). Therefore, the normal development of arterioles was impaired.

Capillary loops begin sprouting from superficial PCP during weeks 4–5 after birth and are complete prior to 9 months of age as perpendicular hairpin-shaped loops projecting into the dermal papillae.[22] Capillary loops in infant and paediatric PWS are not completely developed. In infant and paediatric patients with PWS, the density of papillae containing capillary loops to total papillae per mm of epidermis significantly decreased from 0–1 and 2–10 years of age, respectively (Fig. 2f–h, Table 2). In adolescent and adult PWS, this decrease was even more profound than in infant and paediatric PWS lesions, with significantly lower densities than those in normal human skin at 11–60 years of age (Fig. 2h, Table 2). The ratio of papillae containing capillary loops to total rete ridges per mm epidermis was significantly lower than normal controls (Table 2). The formation of Rete ridges appeared morphologically normal in infantile PWS, but the densities per mm epidermis were significantly reduced during the progression of the disease (Fig. 2g, Table 2), especially in hypertrophic and nodular PWS (Fig. 2i).

The morphological abnormalities observed in vasculatures and deficiency of capillary loop formation in infantile and paediatric PWS suggest that ECs are immature and/or malfunctioned and thus unable to form normal vasculatures, which subsequently fail to form normal capillary loops within the dermal papillae after birth. This rationale led us to investigate the differentiation status of PWS ECs. Next, we found that most infant, paediatric and adult PWS blood vessels except nodules were positive for CD133 and CD166, markers of EPCs (Fig. 3, Table 2). CD133 and CD166 were weakly positive in normal dermal ECs in infantile skin but negative in adult human skin (Fig. 3, Table 2). Consequently, PWS ECs in non-nodular lesions were $CD133^+/CD166^+$ EPCs. The PWS EPCs also showed expression of EC differential markers, for example CD31 and vWF (Fig. 3), suggesting that these EPCs are late-stage EPCs with some initial differentiation occurring. Therefore, the ectatic PWS vasculatures are composed of aberrant late-stage EPCs. Our results suggest that the immaturity of late-stage PWS EPCs accounts for the progressive vascular dilatation observed over time and the reduction in the number of capillary loops formed in the skin.

We then determined the molecular identities of PWS EPCs using specific venous (EphB1, EphB4) and arterial (EfnB2) markers. Their mutually exclusive expression is required during the early stages of normal vascular plexus remodelling.[23–26] PCP also express EphB1.[27] We found that most infant, paediatric and adult PWS ECs co-expressed EphB1 and EfnB2 (n

= 27 patients with PWS; Fig. 4a, b, e; Table 2). We did not observe obvious expression of EphB4 in the PWS sections. A mild immunoreactive signal of EphB1 and EphB4 could be observed in mature veins but not in other types of vasculatures in normal control skin dermis (n = 9 participants; Fig. 4c, d). Normal dermal capillary ECs show a mild EfnB2 immunoreactive signal (Table 3). These data suggest that both arteriole and venous differentiation from PCP are impaired in PWS. PCP is thought to be predetermined to develop into a vein if expression of EphB1 remains, whereas PCP will differentiate into arteries when EphB1 is off and EfnB2 is switched on.[27] Therefore, aberrant PWS PCP with dual expression of EphB1 and EfnB2 may hamper the normal differentiation of both arterioles and venules, eventually resulting in PWS venule-like vasculatures.

In order to explore the roles of co-expressed EphB1/EfnB2 in the alteration of vasculatures, we isolated a subset of normal hDMVECs with high expression of surface EphB1 via biotinylated chimera EfnB2–Fc and streptavidin-conjugated magnetic beads. The rationale for this selection was that the EfnB2–Fc chimera ligand binds to the $EphB1^+/EphB4^+$-expressing venous hDMVEC subpopulation, whereas the remaining arterial hDMVEC subpopulation ($EphB1^-/EphB4^-$) expresses EfnB2. Indeed, the expression of EphB1, EphB4 and EfnB2 could be observed in the heterogeneous population of hDMVECs (Fig. 4k). The EfnB2–Fc selected hDMVEC subpopulation showed a higher level of EphB1 mRNA by a factor of 1·277 ± 0·064 and a much lower level of EfnB2 mRNA by a factor of 0·195 ± 0·021 than nonselected heterogeneous hDMVEC populations (n = 4; Fig. 4f). The protein levels of EfnB2 in the EfnB2–Fc selected hDMVEC subpopulation were undetectable by immunoblotting assay (Fig. 4k). Thus, we designated the selected subpopulation as $EphB1^+/EfnB2^-$ hDMVECs. The remaining hDMVEC subpopulation after EfnB2–Fc selection showed EfnB2 expression but not EphB1 and EphB4, and was designated as $EphB1^-/EphB4^-/EfnB2^+$ hDMVEC subpopulation (Fig. 4k). Subsequently, the $EphB1^+/EfnB2^-$ hDMVECs (n = 4) were transfected with a plasmid carrying EGFP and EfnB2–His. The cells were screened with G418 to obtain $EphB1^+/EGFP^+$ and $EphB1^+/EfnB2^+$ subsets (n = 4 for each cell model) (Fig. 4f). The EGFP-transfected hDMVECs, $EGFP^+/EphB1^+/EfnB2^-$, showed similar EphB1 and EfnB2 mRNA levels to the $EphB1^+/EfnB2^-$ hDMVEC subpopulation (n = 4; Fig. 4f), whereas EfnB2-transfected hDMVECs showed an increase in EfnB2 mRNA by a factor of 3·539 ± 0·372 vs. the $EphB1^+/EfnB2^-$ hDMVEC subpopulation (n = 4; Fig. 4f). Therefore, these cells were designated as $EphB1^+/EfnB2^+$ hDMVECs.

CLS formation has been used to assess morphological differentiations involving multiple cellular signalling-activated processes, including cell migration, adhesion, protease secretion and alignment among a variety of ECs.[28] We performed Matrigel tube formation *in vitro* to characterize the phenotypes of vasculatures formed by various ECs subpopulations prepared as described above. We found that forced co-expression of EphB1/EfnB2 resulted in formation of PWS blood vessel-like capillary tubes at 12–16 h after cell plating, for example significantly thicker branches (Fig. 4g, j), larger branch point areas (Fig. 4h, j) and larger diameters (Fig. 4i, j), in Matrigel compared with wild-type and $EGFP^+$ hDMVECs (Fig. 4b–e). The EphB1/EfnB2 cells formed in the CLS remained dynamically unstable and at 16–20 h tended to aggregate as spheres at the branching points (data not shown). Overexpression of EfnB2 in hDMVECs was confirmed by Western blot using an anti-EfnB2 antibody (Fig. 4k). An immunoprecipitation assay showed that EphB1 and EfnB2 were associated with each

other (Fig. 4k). Taken together, the co-expression of EphB1 and EfnB2 in ECs results in disruption of the normal vasculature and directly contributes to the formation of abnormal PWS-like vasculatures.

Discussion

Although currently largely elusive, there are at least two major hypotheses regarding the pathogenesis of PWS – nerve denervation and genetic mutations. PWS usually show a deficiency in nerve innervation, which has been speculated to be the cause of these abnormal hypervascular skin lesions.[29–31] How- ever, confirmatory evidence for this hypothesis has yet to be obtained. Recent studies have suggested that sporadic somatic mutations of *GNAQ* (c.548G > A) and phosphatidylinositol 3-kinase are linked to the vascular malformations observed in PWS.[12,13,32] Couto *et al.* and Tan et al. further identified that GNAQ (c.548G > A) is primarily present in abnormal PWS blood vessels (60%),[14,15] and/or in connective tissue (30%)[15] and hair follicle/glands (20%).[15] These data suggest that pluripotent cells with GNAQ (c.548G>A) may give rise to multilineages in PWS.[15] In addition, our recent work analysing the pathology of infantile PWS has shown that the entire physiological milieu of human skin is altered during the early course of PWS, including the vasculature and connective tissue.[33] Taken together, our present data, along with these previous reports, suggest that PWS is a multifactorial disease involving not only the vasculature, but also other structures within the dermis.

PWS are usually characterized by a dilatation of postcapillary venules based on morphological observations.[11] Our data herein demonstrated that there were no normal – phenotypically and morphologically – arterioles and venules in PWS skin. PWS blood vessels have $CD133^+/CD166^+/EphB1^+/EfnB2^+$ phenotypes, likely due to differentiation impairments in EPCs. Therefore, our data suggest that the current pathoanatomical descriptions of PWS should be redefined as ‘progressive dilatation of venule-like vasculatures’. During development, both dermal arterioles and venules are differentiated from PCP.[22,27] A recent study suggests that turning off EphB1 and switching on EfnB2 is crucial for dermal PCP differentiation into arterioles. In default mode, PCP is thought to develop into a vein with consistent expression of EphB1.[27] This evidence allows us to speculate that the coexistence of EphB1 and EfnB2 in PWS EPCs will inhibit normal differentiation of both arterioles and venules from PCP, resulting in a venule-like vasculature that is a predetermined fate of PCP. In addition, as Efns and Ephs play a fundamental role in cell–cell interactions, such as the establishment of the arterial–venous vasculature,[23,26] we postulate that the coexistence of EphB1and EfnB2 in ECs will disrupt normal cell–cell interactions and communications, which likely contributes to the progressive dilatation of PWS vasculatures. Indeed, our data showed that forced co-expression of EphB1 and EfnB2 in normal ECs leads to formation of PWS-like vasculatures *in vitro*, for example large-diameter and thick-wall capillaries. These data directly support our hypothesis.

In general, Efn interacts with Eph on adjacent cells, inducing Eph receptor forward and Efn ligand reverse signalling.[34,35] Elevation of Eph forward signalling promotes cell segregation; an increase in Efn reverse signalling facilitates neoangiogenesis and invasion.[35–39] In addition, autoregulation of Eph and Efn signalling occurs when both are expressed in some

cell types.[36,40] A '*cis*-binding' theory has been proposed by several reports; namely, that co-expression of Eph and Efn will attenuate Eph forward signalling via lateral *cis*-binding properties not involving the ligand binding domain of Eph.[41–43] In the current study, we have shown that EphB1 and EfnB2 are associated, which results in a PWS-like vasculature phenotype, which probably acts through the *cis*-binding mechanism. However, how the cis-binding mechanism regulates EphB1 forward and/or EfnB2 reverse signalling is yet to be determined in our cell models, which will be the goal of future studies.

In addition to developmental tissue morphogenesis, there is increasing evidence that Eph–Efn signalling regulates cell differentiation, as well as controls stem cell positioning and proliferation. For example, EfnB2 reverse signalling can inhibit osteoclast differentiation, whereas EphB4 forward signalling promotes osteoblast differentiation.[44] The roles of Eph–Efn signalling in the modulation of progenitor cell proliferation and differentiation are largely diverse, presumably depending on downstream effectors, such as activation or inhibition of the mitogen-activated protein kinase pathway.[45–47] In the current study, we have shown that PWS ECs are differentiation-impaired EPCs with phenotypes of $CD133^{+}$/$CD166^{+}$/$EphB1^{+}$/$EfnB2^{+}$, suggesting the potential roles of co-expression of EphB1/EfnB2 in regulation of differentiation status of PWS EPCs. However, the detailed mechanisms remain obscure. Nevertheless, the characterization of differentiation status of PWS EPCs is of clinical significance, such as therapeutic targeting of EphB1/EfnB2 signalling to modulate the differentiation process of PWS EPCs.

In summary, PWS blood vessels are immature capillary vasculatures with aberrant stemness properties and dual venous and arterial identities. We conclude that PWS is a disease resulting from differentiation-impaired EPCs in human skin that develop into venule-like vasculatures morphologically and undergo progressive dilatation due to the disruption of normal EC–EC interactions by the co-existence of EphB1/EfnB2.

Supplementary Material

Refer to Web version on PubMed Central for supplementary material.

Acknowledgments

Institutional support was provided by the Arnold and Mabel Beckman Foundation and the David and Lucile Packard Foundation. We greatly appreciate the Sue & Bill Gross Stem Cell Research Center at the University of California, Irvine, for their assistance with the histology image-acquisition process experiments.

Funding sources

This work was supported by grants from the National Institutes of Health (AR063766 to W.T.; HL70562 to D.-B.C.; AR47551 and AR59244 to J.S.N.) and research grants (F03.12 and F01.13 to W.T.) from the American Society for Laser Medicine and Surgery and National Natural Scientific Foundation of China (81301355 to L.G. and 81271773 to H.L.). Any views expressed here represent personal opinion and do not necessarily reflect those of the U.S. Department of Health and Human Services or the United States federal government.

References

1. Jacobs AH, Walton RG. The incidence of birthmarks in the neonate. Pediatrics 1976; 58:218–22. [PubMed: 951136]
2. Pratt AG. Birthmarks in infants. Arch Dermatol Syphilol 1953; 67:302–5.

3. Geronemus RG, Ashinoff R. The medical necessity of evaluation and treatment of port-wine stains. J Dermatol Surg Oncol 1991; 17:76–9. [PubMed: 1991884]
4. Lever WF, Schaumburg-Lever G. Histopathology of the Skin, 7th edn. Philadelphia, PA: JB Lippincott, 1990.
5. Kalick SM. Toward an interdisciplinary psychology of appearances. Psychiatry 1978; 41:243–53.
6. Heller A, Rafman S, Zvagulis I, Pless IB. Birth-defects and psychosocial adjustment. Am J Dis Child 1985; 139:257–63. [PubMed: 3976606]
7. Malm M, Carlberg M. Port-wine stain – a surgical and psychological problem. Ann Plast Surg 1988; 20:512–6. [PubMed: 3389703]
8. Gao L, Phan S, Nadora DM et al. Topical rapamycin systematically suppresses the early stages of pulsed dye laser-induced angiogenesis pathways. Lasers Surg Med 2014; 46:679–88. [PubMed: 25270513]
9. Gao L, Nadora DM, Phan S et al. Topical axitinib suppresses angiogenesis pathways induced by pulsed dye laser. Br J Dermatol 2015; 172:669–76. [PubMed: 25283693]
10. Tan W, Jia W, Sun V et al. Topical rapamycin suppresses the angiogenesis pathways induced by pulsed dye laser: molecular mechanisms of inhibition of regeneration and revascularization of photocoagulated cutaneous blood vessels. Lasers Surg Med 2012; 44:796–804. [PubMed: 23213008]
11. Schneider BV, Mitsuhashi Y, Schnyder UW. Ultrastructural observations in port wine stains. Arch Dermatol Res 1988; 280:338–45. [PubMed: 3190266]
12. Hashizume H, Baluk P, Morikawa S et al. Openings between defective endothelial cells explain tumor vessel leakiness. Am J Pathol 2000; 156:1363–80. [PubMed: 10751361]
13. Shirley MD, Tang H, Gallione CJ et al. Sturge–Weber syndrome and port-wine stains caused by somatic mutation in GNAQ. N Engl J Med 2013; 368:1971–9. [PubMed: 23656586]
14. Couto JA, Huang L, Vivero MP et al. Endothelial cells from capillary malformations are enriched for somatic GNAQ mutations. Plast Reconstr Surg 2016; 137:77e–82e.
15. Tan W, Nadora DM, Gao L et al. The somatic GNAQ mutation (R183Q) is primarily located in port wine stain blood vessels. J Am Acad Dermatol 2016; 74:380–3. [PubMed: 26775782]
16. Tan W, Chernova M, Gao L et al. Sustained activation of c-Jun N-terminal and extracellular signal-regulated kinases in port-wine stain blood vessels. J Am Acad Dermatol 2014; 71:964–8. [PubMed: 25135651]
17. Yen A, Braverman IM. Ultrastructure of the human dermal microcirculation: the horizontal plexus of the papillary dermis. J Invest Dermatol 1976; 66:131–42. [PubMed: 1249441]
18. Populo H, Vinagre J, Lopes JM, Soares P. Analysis of GNAQ mutations, proliferation and MAPK pathway activation in uveal melanomas. Br J Ophthalmol 2011; 95:715–9. [PubMed: 20805136]
19. Goodwin AM. In vitro assays of angiogenesis for assessment of angiogenic and anti-angiogenic agents. Microvasc Res 2007; 74:172–83. [PubMed: 17631914]
20. Kubota Y, Kleinman HK, Martin GR, Lawley TJ. Role of laminin and basement membrane in the morphological differentiation of human endothelial cells into capillary-like structures. J Cell Biol 1988; 107:1589–98. [PubMed: 3049626]
21. Johnson CL, Holbrook KA. Development of human embryonic and fetal dermal vasculature. J Invest Dermatol 1989; 93:10S–17S. [PubMed: 2666515]
22. Perera P, Kurban AK, Ryan TJ. The development of the cutaneous microvascular system in the newborn. Br J Dermtol 1970; 82:86–91.
23. Adams RH, Wilkinson GA, Weiss C et al. Roles of ephrinB ligands and EphB receptors in cardiovascular development: demarcation of arterial/venous domains, vascular morphogenesis, and sprouting angiogenesis. Genes Dev 1999; 13:295–306. [PubMed: 9990854]
24. Gerety SS, Anderson DJ. Cardiovascular ephrinB2 function is essential for embryonic angiogenesis. Development 2002; 129:1397–410. [PubMed: 11880349]
25. Gerety SS, Wang HU, Chen ZF, Anderson DJ. Symmetrical mutant phenotypes of the receptor EphB4 and its specific transmembrane ligand ephrin-B2 in cardiovascular development. Mol Cell 1999; 4:403–14. [PubMed: 10518221]

26. Wang HU, Chen ZF, Anderson DJ. Molecular distinction and angiogenic interaction between embryonic arteries and veins revealed by ephrin-B2 and its receptor Eph-B4. Cell 1998; 93:741–53. [PubMed: 9630219]
27. Li W, Mukouyama YS. Tissue-specific venous expression of the EPH family receptor EphB1 in the skin vasculature. Dev Dyn 2013; 242:976–88. [PubMed: 23649798]
28. Arnaoutova I, George J, Kleinman HK, Benton G. The endothelial cell tube formation assay on basement membrane turns 20: state of the science and the art. Angiogenesis 2009; 12:267–74. [PubMed: 19399631]
29. Rydh M, Malm M, Jernbeck J, Dalsgaard CJ. Ectatic blood vessels in port-wine stains lack innervation: possible role in pathogenesis. Plast Reconstr Surg 1991; 87:419–22. [PubMed: 1825517]
30. Selim MM, Kelly KM, Nelson JS et al. Confocal microscopy study of nerves and blood vessels in untreated and treated port wine stains: preliminary observations. Dermatol Surg 2004; 30:892–7. [PubMed: 15171768]
31. Tallman B, Tan OT, Morelli JG et al. Location of port-wine stains and the likelihood of ophthalmic and/or central nervous system complications. Pediatrics 1991; 87:323–7. [PubMed: 1805804]
32. Luks VL, Kamitaki N, Vivero MP et al. Lymphatic and other vascular malformative/overgrowth disorders are caused by somatic mutations in PIK3CA. J Pediatr 2015; 166:1048–54. [PubMed: 25681199]
33. Tan W, Zakka LR, Gao L et al. Pathological alterations involve the entire skin physiological milieu in infantile and early childhood port wine stain. Br J Dermatol 2017; 177:293–6. [PubMed: 27639180]
34. Himanen JP, Saha N, Nikolov DB. Cell–cell signaling via Eph receptors and ephrins. Curr Opin Cell Biol 2007; 19:534–42. [PubMed: 17928214]
35. Nievergall E, Lackmann M, Janes PW. Eph-dependent cell-cell adhesion and segregation in development and cancer. Cell Mol Life Sci 2012; 69:1813–42. [PubMed: 22204021]
36. Dvorak AM, Mihm MC Jr, Dvorak HF. Morphology of delayedtype hypersensitivity reactions in man. II. Ultrastructural alterations affecting the microvasculature and the tissue mast cells. Lab Invest 1976; 34:179–91. [PubMed: 1249919]
37. Lackmann M, Boyd AW. Eph, a protein family coming of age: more confusion, insight, or complexity? Sci Signal 2008; 1:re2.
38. Daar IO. Non-SH2/PDZ reverse signaling by ephrins. Semin Cell Dev Biol 2012; 23:65–74. [PubMed: 22040914]
39. Davy A, Soriano P. Ephrin signaling in vivo: look both ways. Dev Dyn 2005; 232:1–10. [PubMed: 15580616]
40. Pasquale EB. Eph receptor signalling casts a wide net on cell behaviour. Nat Rev Mol Cell Biol 2005; 6:462–75. [PubMed: 15928710]
41. Janes PW, Adikari S, Lackmann M. Eph/ephrin signalling and function in oncogenesis: lessons from embryonic development. Curr Cancer Drug Targets 2008; 8:473–9. [PubMed: 18781894]
42. Kao TJ, Kania A. Ephrin-mediated cis-attenuation of Eph receptor signaling is essential for spinal motor axon guidance. Neuron 2011; 71:76–91. [PubMed: 21745639]
43. Marquardt T, Shirasaki R, Ghosh S et al. Coexpressed EphA receptors and ephrin-A ligands mediate opposing actions on growth cone navigation from distinct membrane domains. Cell 2005; 121:127–39. [PubMed: 15820684]
44. Zhao C, Irie N, Takada Y et al. Bidirectional ephrinB2-EphB4 signaling controls bone homeostasis. Cell Metab 2006; 4:111–21. [PubMed: 16890539]
45. Jiao JW, Feldheim DA, Chen DF. Ephrins as negative regulators of adult neurogenesis in diverse regions of the central nervous system. Proc Natl Acad Sci U S A 2008; 105:8778–83. [PubMed: 18562299]
46. Aoki M, Yamashita T, Tohyama M. EphA receptors direct the differentiation of mammalian neural precursor cells through a mitogen-activated protein kinase-dependent pathway. J Biol Chem 2004; 279:32643–50. [PubMed: 15145949]
47. Wilkinson DG. Regulation of cell differentiation by Eph receptor and ephrin signaling. Cell Adh Migr 2014; 8:339–48. [PubMed: 25482623]

What's already known about this topic?

- Port-wine stain (PWS) is a congenital progressive vascular malformation of human skin.
- Vascular lesions are considered as dilation of postcapillary venules in PWS.
- Pathological alterations involving the entire physiological milieu of skin are present in the early stage of PWS.

What does this study add?

- PWS endothelial cells (ECs) are differentiation-impaired, late-stage endothelial progenitor cells (EPCs) with a phenotype of $CD133^{+}$/$CD166^{+}$/Eph receptor B1 $(EphB1)^{+}$/ephrin B2 $(EfnB2)^{+}$.
- PWS blood vessels are immature venule-like pathoanatomical vasculatures.
- Coexistence of EphB1 and EfnB2 in PWS ECs contributes to the progressive dilatation of PWS vasculatures.

What is the translational message?

- PWS EPCs are the major contributor to the angiogenesis of PWS blood vessels after pulsed-dye laser therapy.
- The surface markers EphB1, EfnB2, CD133 and CD166 provide a molecular basis for specific targeting of PWS EPCs.
- Blockage of EphB1/EfnB2 signalling may promote PWS EPC differentiation and inhibit progressive dilatation of PWS vasculatures

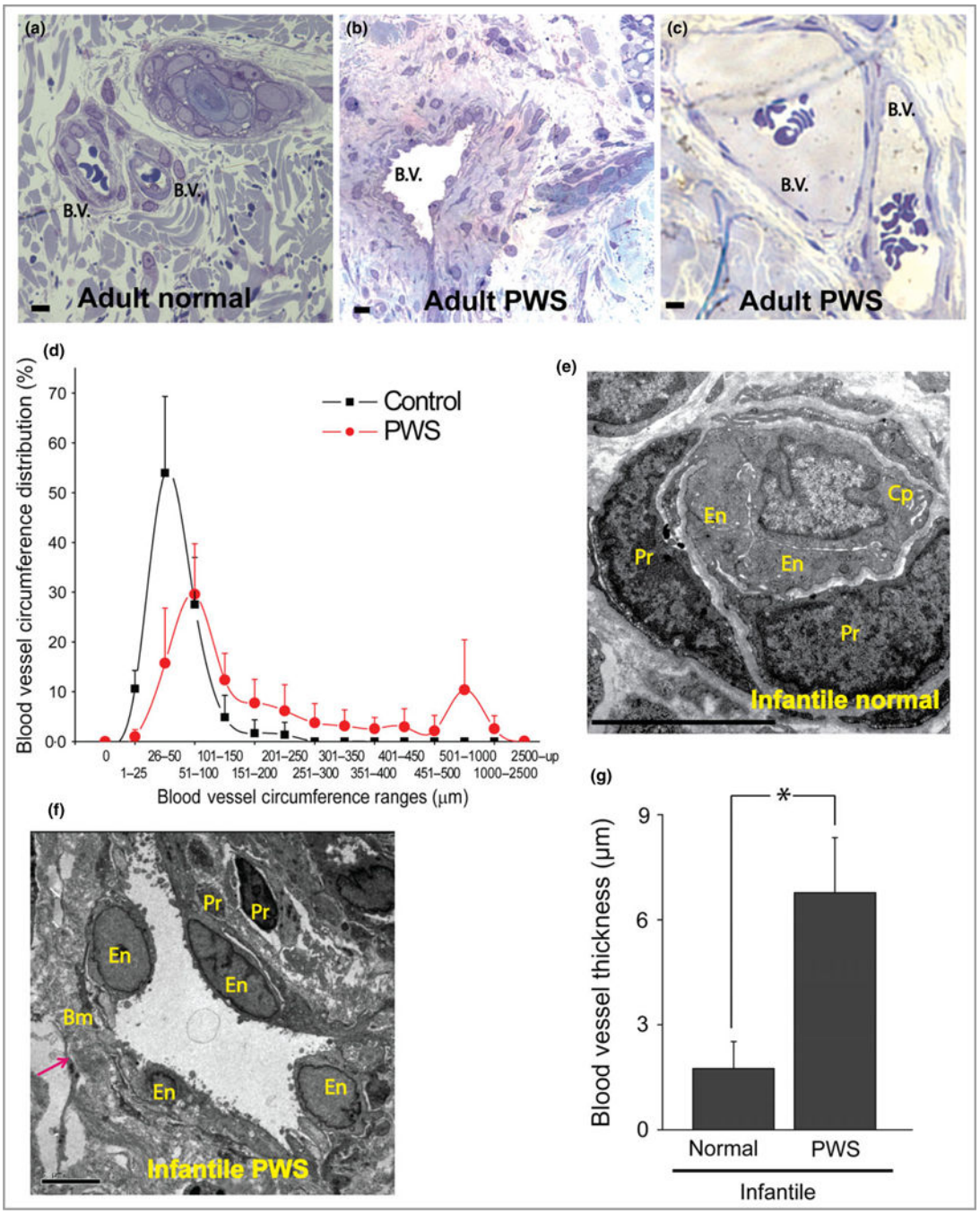

Fig 1.

Thick- and thin-walled blood vessels in adult and infant port-wine stain (PWS) lesions. (a) Normal blood vessels (b.v.) in adjacent normal skin from an adult with PWS. (b, c) Thick- and thin-walled PWS blood vessels from adults with PWS. (d) PWS blood vessel circumference distribution vs. normal dermal vasculatures (four patients with PWS and four normal adult participants). (e) Electron microscopy (EM) showed a normal capillary in adjacent normal skin from an infant with PWS. En, endothelial cell; Pr, pericyte; Cp, capillary. (f) EM showed an ectatic, thick-walled blood vessel with replication of the

basement membranes in PWS from the same subject as in (e). Bm, basement membrane. The arrow indicates the blood vessel wall. (g) Infantile PWS blood vessels showed a significantly thicker blood vessel wall compared with normal dermal blood vessels from the same subjects ($n = 4$). Scale bar = 5 μm. *$P < 0{\cdot}05$ vs. control.

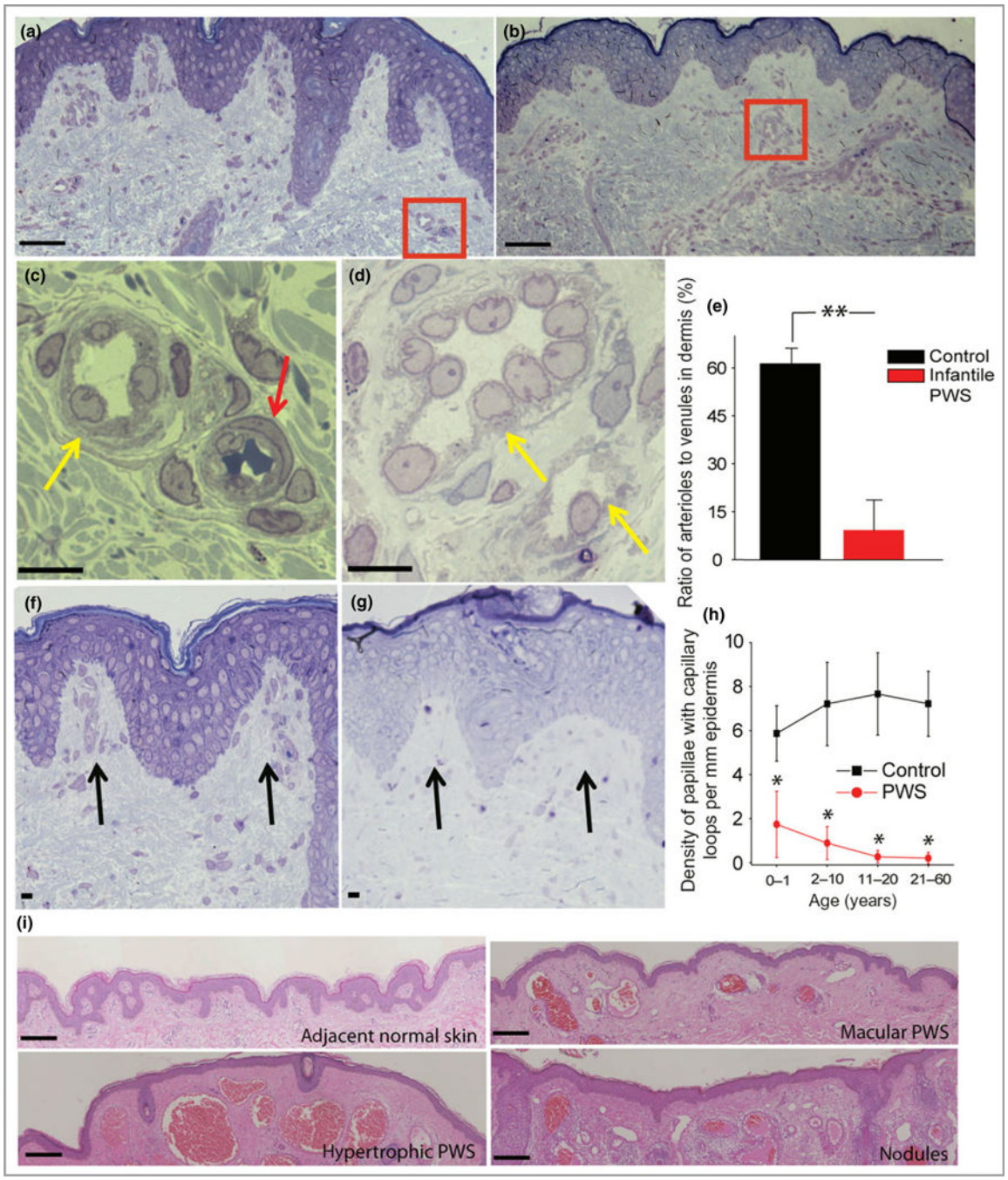

Fig 2.

Multiple developmental impairments of infant port-wine stain (PWS) vasculatures. (a) Semi-thin section showed normal adjacent skin from an infant with PWS. (b) Semi-thin section showed PWS lesional skin from the same subject as in (a). Scale bar = 20 lm. (c) A normal venule (yellow arrow) and arteriole (red arrow) from the red-boxed area in (a). (d) PWS pathoanatomical venule-like vasculatures (yellow arrows) from the red-boxed area in (b). Scale bar = 5 μm. (e) The ratio of arteriole to venule-like vasculatures in infantile PWS lesions was significantly reduced compared with normal adjacent skin from the same

subjects ($n = 4$). (f) Normal formation of capillary loop (black arrows) in adjacent normal skin from an infant with PWS. (g) Defects in capillary loop formation along with normal development of epidermal rete ridges in PWS from the same subject as in (d). Scale bar = 5 μm. (h) Quantitative analysis of the density of papillae containing capillary loops per mm epidermis in patients with PWS vs. normal subjects among groups of different ages. (i) Reduction of capillary loops and rete ridges in PWS flat reddish macular, protuberant hypertrophic areas and nodules from the same subject. Scale bar = 100 μm. $^{**}P < 0{\cdot}01$ and $^{*}P < 0{\cdot}05$ vs. the control groups in (e) and (h).

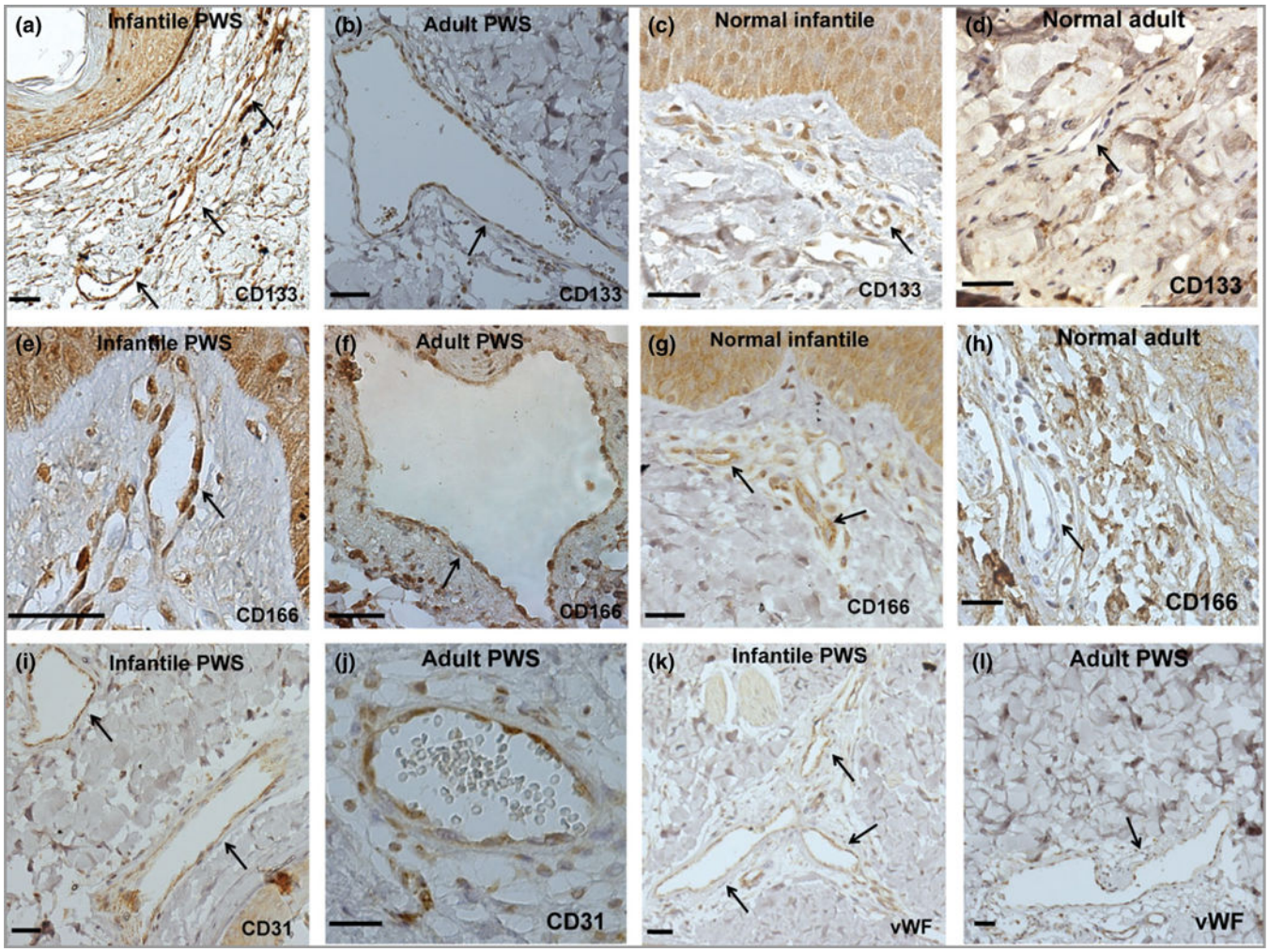

Fig 3.

Port-wine stain (PWS) endothelial cells (ECs) presented stemness phenotypes of $CD133^{+}$/$CD166^{+}$ in non-nodular lesions. (a–h) Expression of CD133 and CD166 in infant and adult PWS and normal subjects. (i–l) PWS ECs expressed EC markers CD31 and von Willebrand factor (vWF). Positive stain is diaminobenzidine (DAB) (brown). Scale bar = 50 μm. Arrows indicate blood vessels.

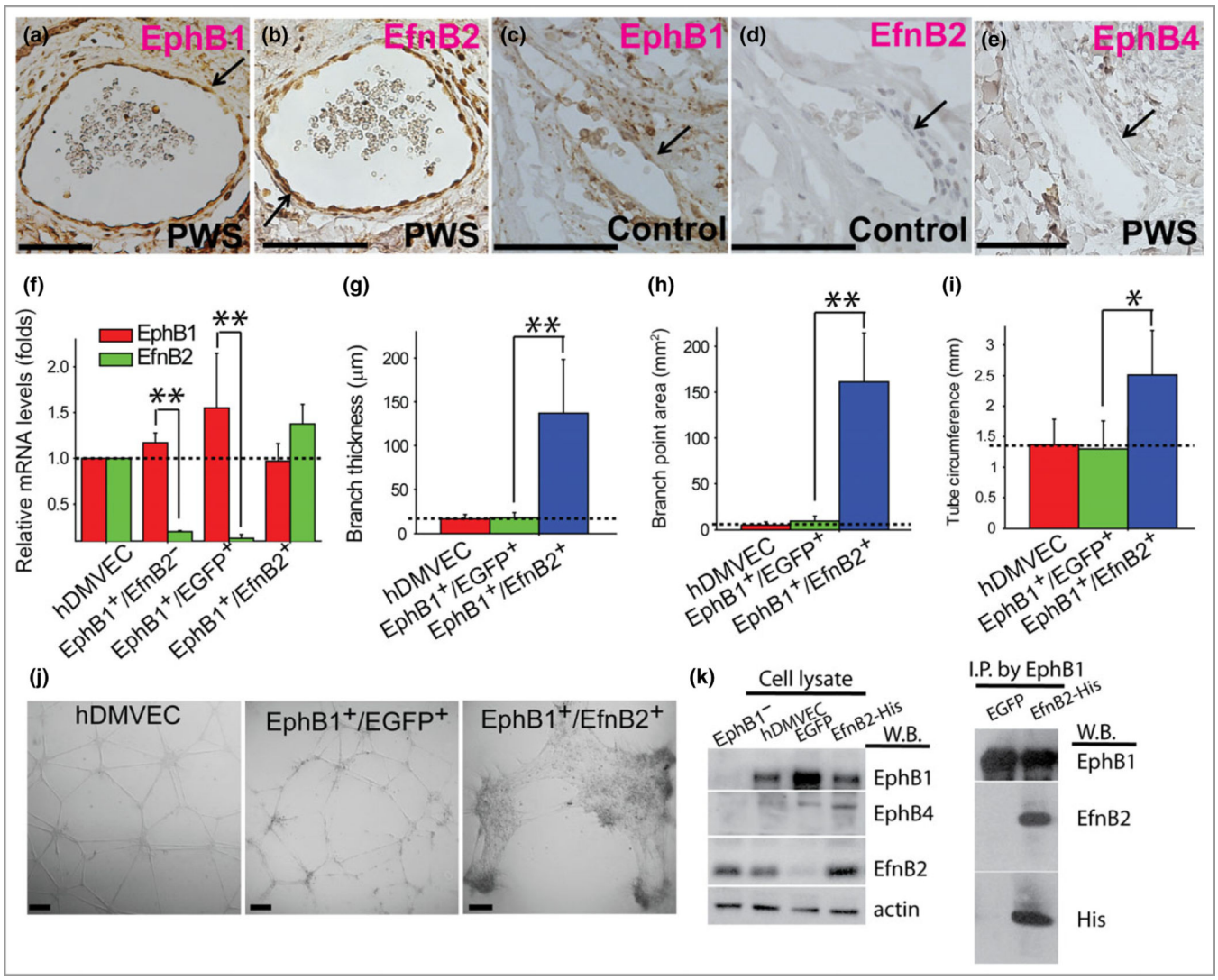

Fig 4.

Port-wine stain (PWS) endothelial cells (ECs) showed dual arterial and venous identities of co-expression of Eph receptor B1 (EphB1) and ephrin B2 (EfnB2). (a, b) PWS ECs were EphB1^{+} and EfnB2^{+}. (c, d) A normal dermal venule showed expression of EphB1 but not EfnB2. (e) PWS ECs were EphB4^{-}. (f) Relative mRNA levels of EphB1 and EfnB2 in selected normal human dermal microvascular endothelial cell (hDMVEC) subtypes. (g–i) Forced co-expression of EphB1 and EfnB2 in normal hDMVECs showed a significant increase in (g) branch thickness, (h) branch point area and (i) tube circumference of the capillary tubes formed in vitro compared with controls. (j) PWS blood vessel-like phenotypes were observed in EphB1^{+}/EfnB2^{+} but not in wild-type and EphB1^{+}/EGFP^{+} control hDMVECs in an *in vitro* capillary tube formation assay at 12 h after cell plating. Positive stain is diaminobenzidine (DAB; brown). Scale bar = 100 μm. *$P < 0{\cdot}05$, ** $P < 0{\cdot}01$ vs. control. The arrows indicate blood vessels. (k) Left panel, detection of expression of EphB1, EphB4, β-actin and EfnB2 by Western blot (W.B.) in various hDMVEC subpopulations. hDMVEC, heterogeneous population prior to EfnB2–Fc selection; EphB1^{-}

hDMVEC, the remaining hDMVEC subpopulation after EfnB2–Fc selection; enhanced green fluorescent protein (EGFP) or EfnB2–His, overexpression of EGFP or EfnB2 in the EfnB2–Fc selected hDMVEC subpopulation. Right panel, an anti-EphB1 antibody was used to immunoprecipitate EphB1 from cell lysate and EfnB2 was detected from the immunoprecipitated protein complex using an anti-EfnB2 or anti-His antibody.

Table 1

Clinical description of patients with port-wine stains (PWS)

Patient no.	Sex	Age (years)	Diagnosis	Treatment history
1	F	0	PWS arm	None
2	F	0	PWS chest	None
3	M	1	PWS face	PDL
4	M	1	PWS face	None
5	M	2	PWS back	None
6	M	2	PWS back	None
7	M	2	PWS face and back	None
8	M	3	PWS face	None
9	F	3	PWS face and back	None
10	M	3	PWS face	None
11	M	3	PWS face	None
12	F	3	PWS face	None
13	F	4	PWS face	None
14	F	5	PWS face	None
15	M	6	PWS arm	None
16	F	16	PWS face	PDL
17	F	13	PWS face	None
18	M	27	PWS face	None
19	M	38	PWS face	PDL
20	M	38	PWS arm	PDL
21	M	41	PWS face	PDL
22	M	51	PWS face	None
23	M	55	PWS face	None
24	F	56	PWS face	PDL
25	F	40	PWS face	None
26	M	55	PWS face	PDL
27	M	36	PWS face	PDL

F, female; M, male; PDL, pulsed-dye laser.

Table 2

Impairment of normal capillary loop formation in patients with port-wine stains (PWS)

	Density of rete ridges[a]		Density of papillae with capillary loops[b]		Ratio[c]		n	
Age group (years)	**Control**	**PWS**	**Control**	**PWS**	**Control**	**PWS**	**Control**	**PWS**
0–1	8.43 ± 1.99	6.86 ± 3.77	5.81 ± 1.26	1.74 ± 1.51 *	0.71 ± 0.09	0.22 ± 0.20 *	14	4
2–10	9.56 ± 2.26	3.71 ± 1.90 *	7.21 ± 1.89	0.89 ± 0.75 *	0.77 ± 0.14	0.25 ± 0.21 *	40	11
11–29	9.90 ± 2.44	1.96 ± 2.16 *	7.66 ± 1.87	0.27 ± 0.28 *	0.78 ± 0.10	0.22 ± 0.22 *	68	5
30–60	9.74 ± 1.79	2.26 ± 3.17 *	7.22 ± 1.48	0.20 ± 0.26 *	0.75 ± 0.15	0.18 ± 0.24 *	20	17

Data are mean ± SD unless otherwise indicated.

[a] Number of rete ridges per mm epidermis;

[b] number of papillae containing capillary loops per mm epidermis;

[c] number of papillae containing capillary loops/number of total rete ridges per mm epidermis.

* $P < 0{\cdot}05$ vs. control groups.

Table 3

Immunoreactive scores of each surface marker in blood vessels from controls and patients with port-wine stains (PWS)

Patient no.	Age/sample		CD133	CD166	EphB1	EfnB2
1	Infant	S	2	3	0	2
2	Infant	T	6	6	6	2
3	Infant	Ex	4	6	6	4
4	Infant	S	3	6	4	4
5	Paediatric	T	4	6	1	3
6	Paediatric	T	6	6	1	4
7	Paediatric	T	4	6	1	4
8	Paediatric	F	4	4	2	2
9	Paediatric	T	4	6	3	2
10	Paediatric	F	4	6	4	3
11	Paediatric	F	6	6	1	3
12	Paediatric	F	3	4	0	1
13	Paediatric	F	4	6	6	4
14	Paediatric	F	4	4	1	2
15	Paediatric	Ex	2	4	4	1
16	Teen.	F	2	4	4	4
		E	2	3	4	4
17	Teenage	F	6	3	3	2
		E	3	2	2	6
18	Adult	F	2	2	4	2
		E	0	0	4	1
19	Adult	Ex	2	2	4	3
20	Adult	S	6	6	0	3
21	Adult	S	0	1	6	0
22	Adult	F	6	6	4	6
		N	6	6	1	4
23	Adult	F	3	3	4	4
		E	2	2	4	4
24	Adult	F	2	2	4	4
		E	0	0	4	0
		D-l	0	0	0	2
		D-2	0	0	4	2
25	Adult	F	2	1	6	1
26	Adult	F	2	0	6	1
27	Adult	F	3	1	4	1
		D	1	0	1	0
Control 1	Paediatric	F	2	1	1	2
Control 2	Paediatric	F	2	2	1	3

Patient no.	Age/sample		CD133	CD166	EphB1	EfnB2
Control 3	Paediatric	Ex	1	1	1	2
Control 4	Paediatric	F	2	3	1	3
Control 5	Adult	Ex	0	0	0	1
Control 6	Adult	Ex	0	0	0	1
Control 7	Adult	F	0	0	0	2
Control 8	Adult	F	0	0	0	3
Control 9	Adult	Ex	0	0	0	2

EphB1, Eph receptor B1; Efn-B2, ephrin B2; S, scalp; T, trunk; Ex, extremity; F, facial; N, neck; E, edge of PWS lesion sites; D, nodular PWS.